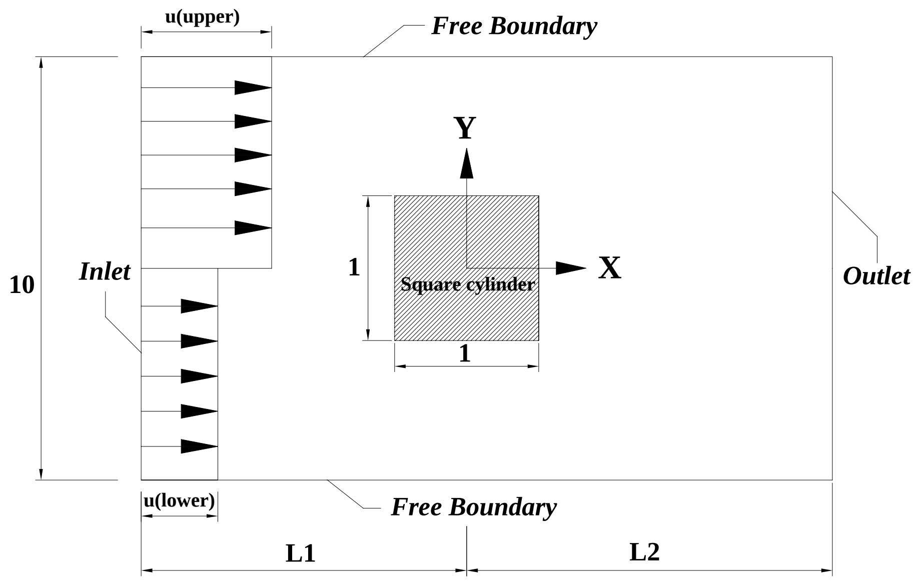

Figure 2-1. Illustration of the physical model. The inlet velocities u(upper) and u(lower) in the figure above equal $1+\alpha$ and $1-\alpha$, respectively.

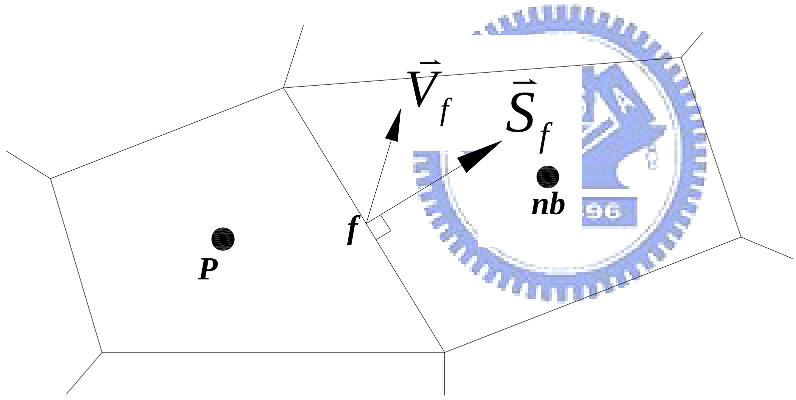

Figure 3-1. Illustration of the primary cell P and the neighbor cell nb with a face *f* in between

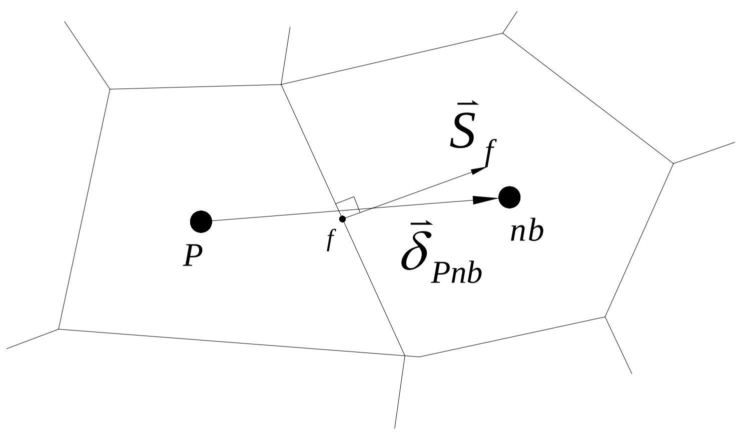

Figure 3-2. Illustration of the primary cell P and the neighbor cell nb with a face *f* in between

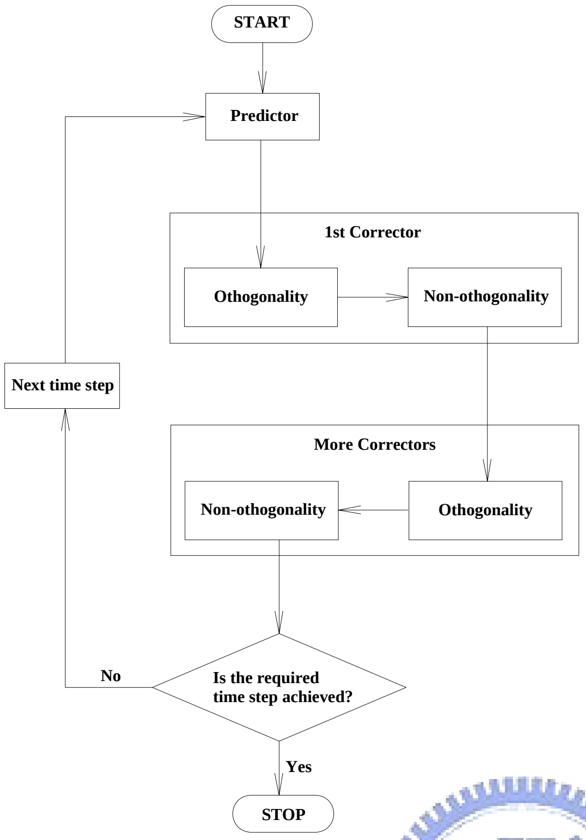

Figure 4-1. Block diagram of solution procedure of PISO algorithm.

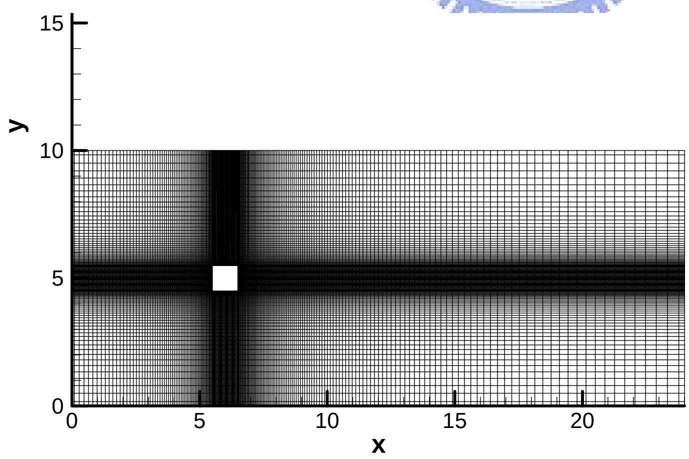

Figure 5-1. The computational mesh and geometry.

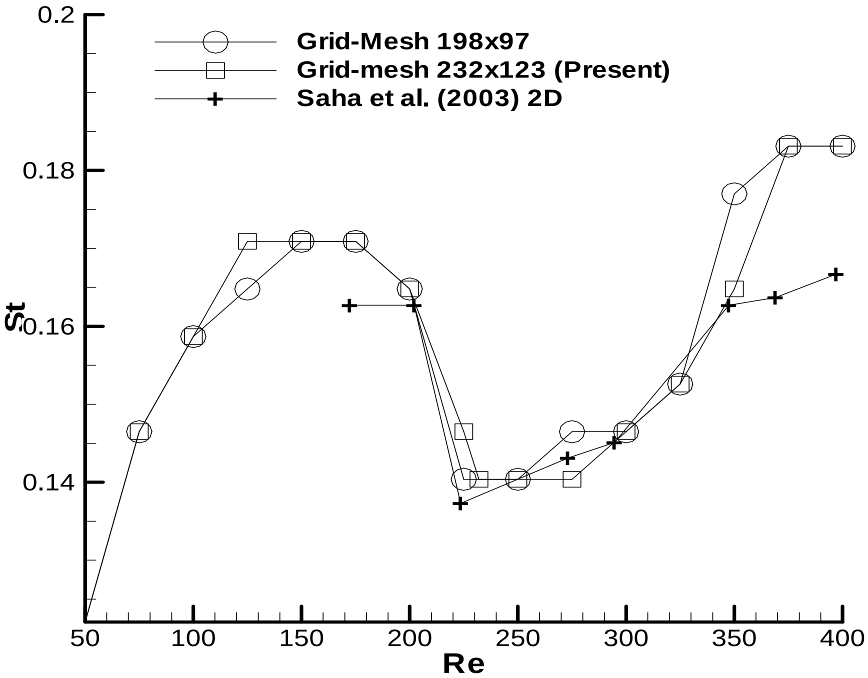

Figure 5-2. Variation of Strouhal number with Reynolds number (Uniform free stream cases of cell numbers 198x97 and 232x123)

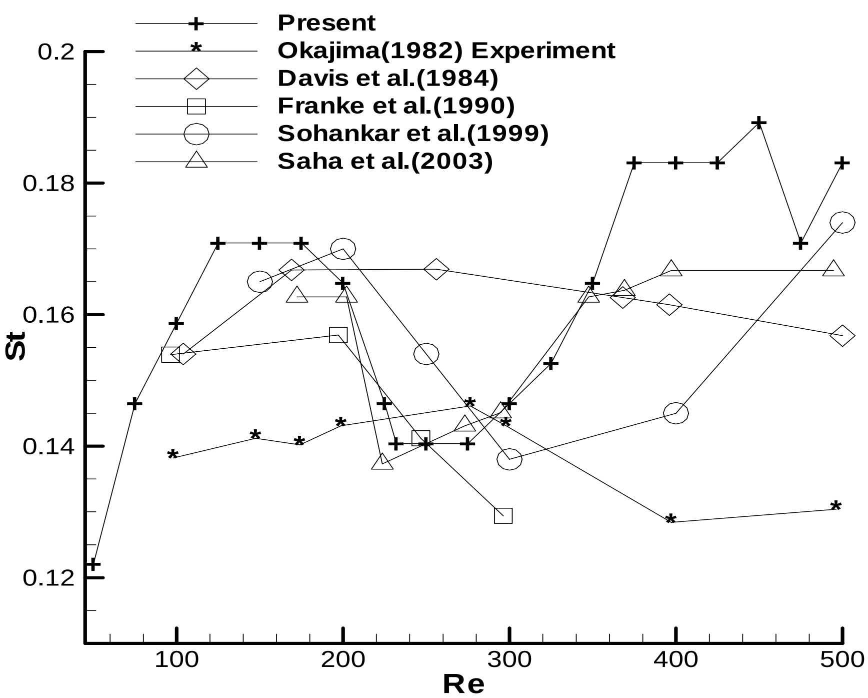

Figure 5-3. Variation of Strouhal number with Reynolds number (Uniform free stream).

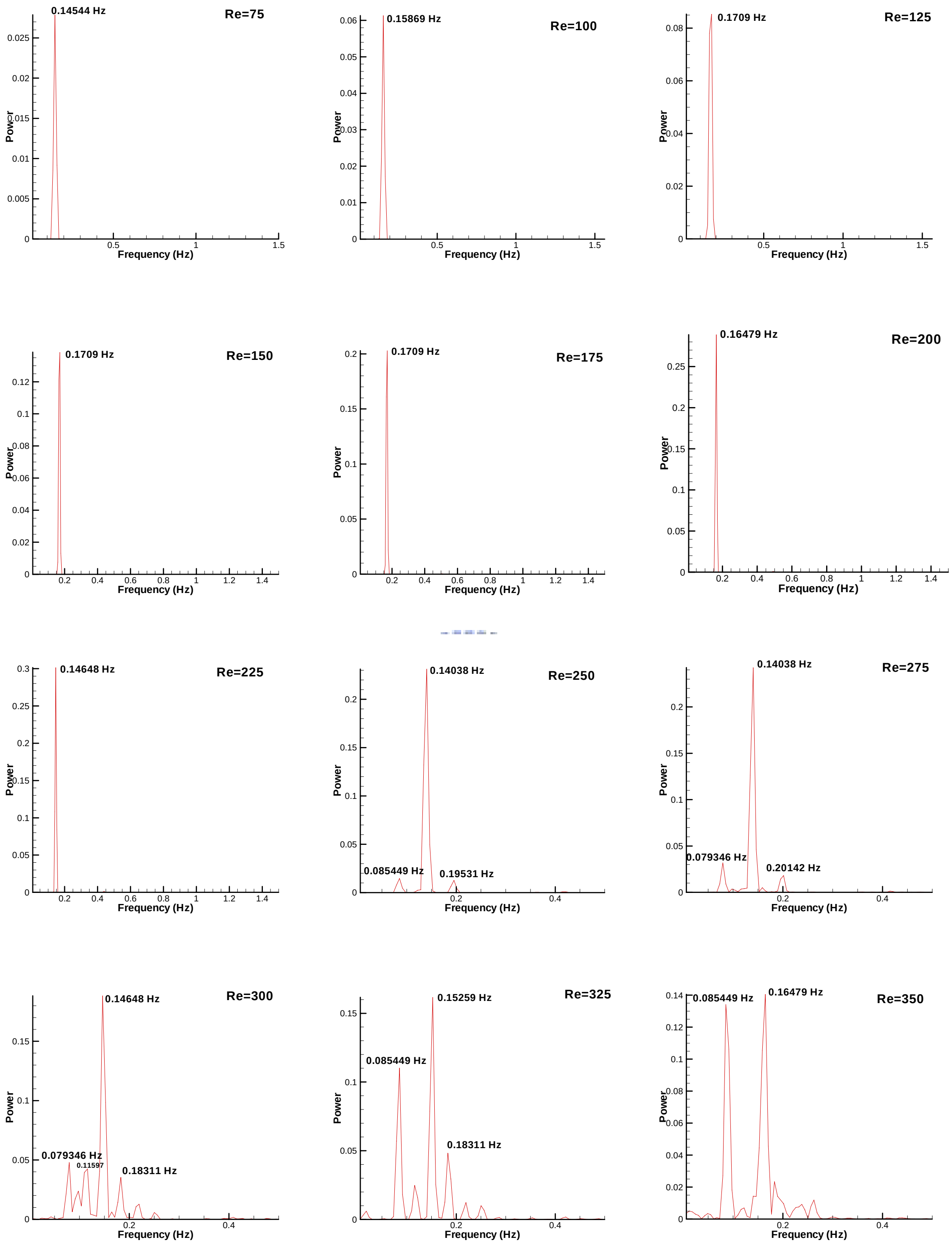

Figure 5-4. Variation of transverse velocity [at point (x, y)= (1.23, 0)] spectra with Reynolds number (Uniform free stream). *Continue…*

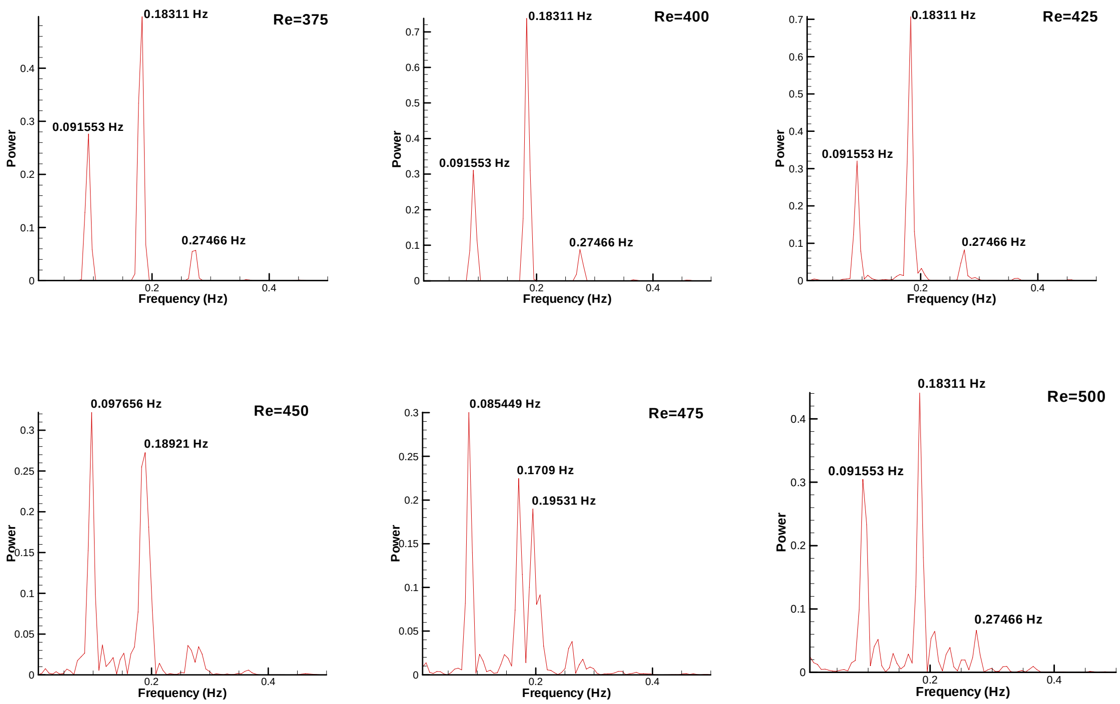

Figure 5-4. Variation of transverse velocity [at point (x, y)= (1.23, 0)] spectra with Reynolds number (Uniform free stream).

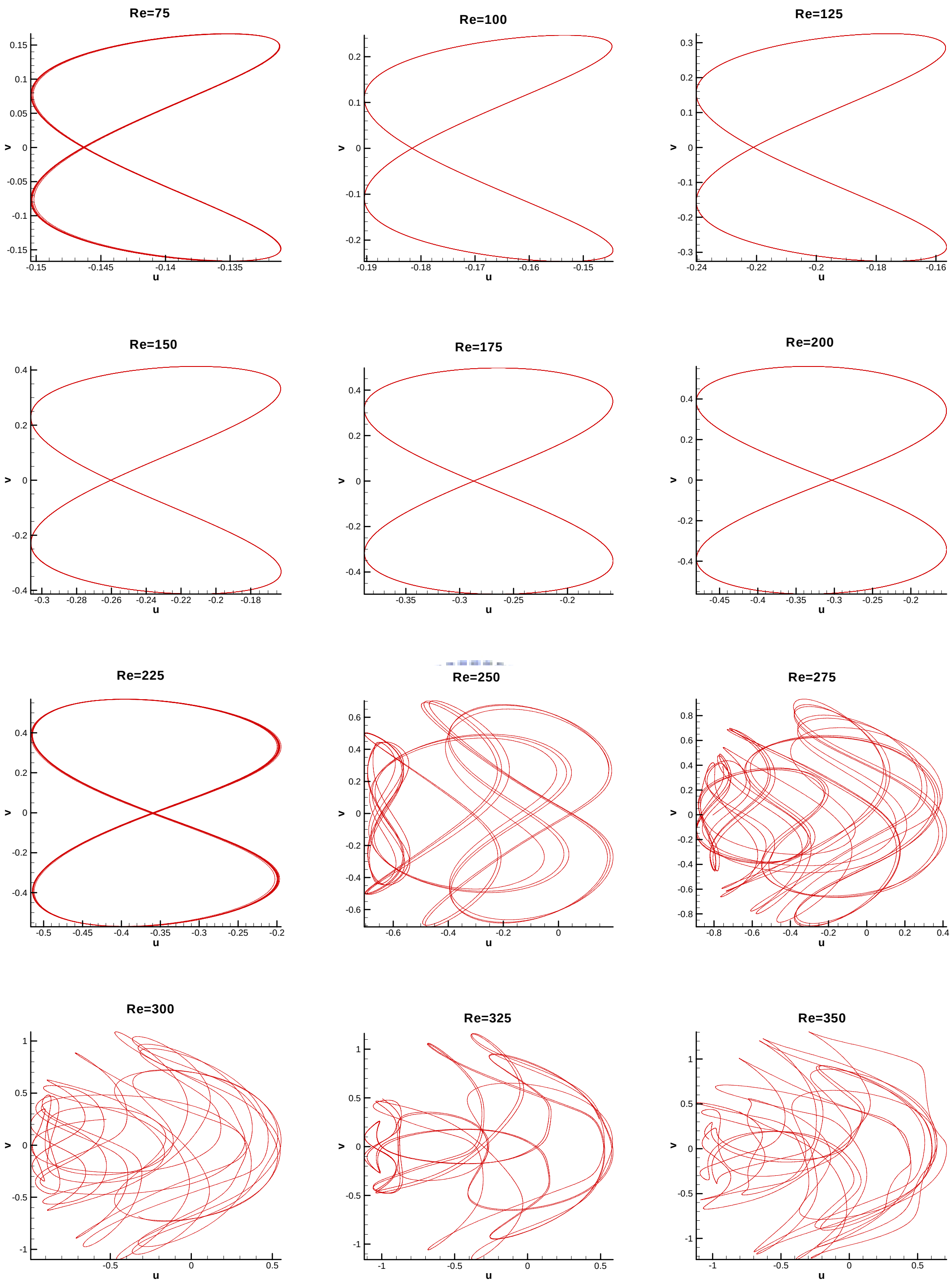

Figure 5-5. Variation of phase space of velocity components at (x=1.23, y=0) with Reynolds number (Uniform free stream). *Continue…*

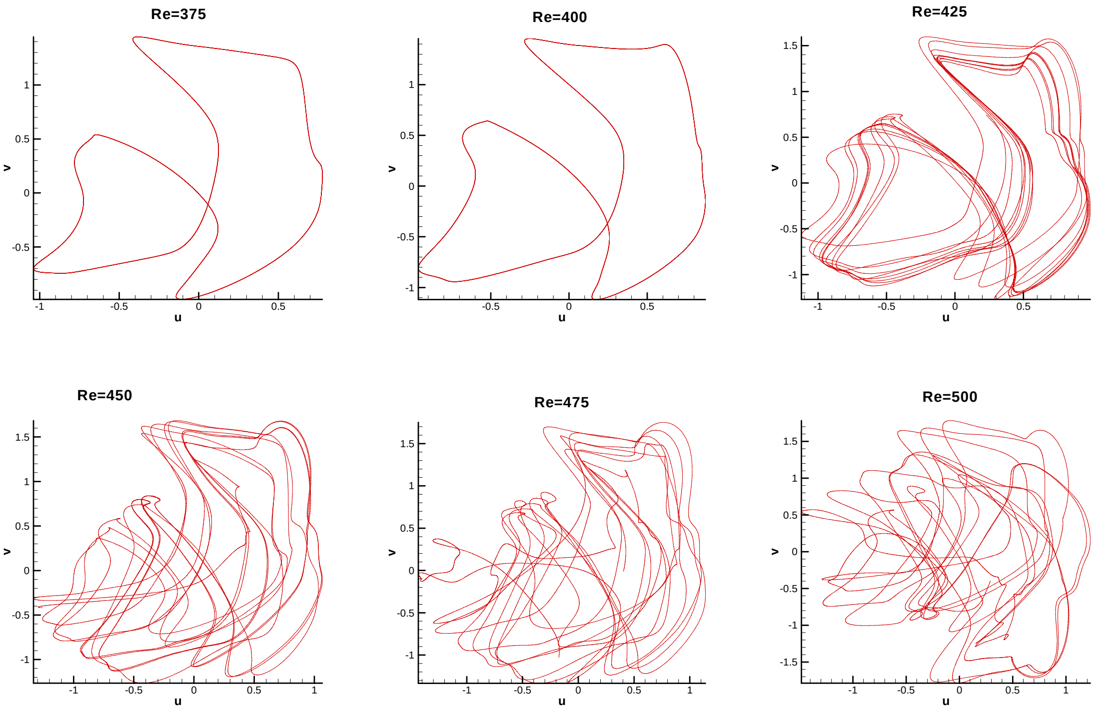

Figure 5-5. Variation of phase space of velocity components at (x=1.23, y=0) with Reynolds number (Uniform free stream).

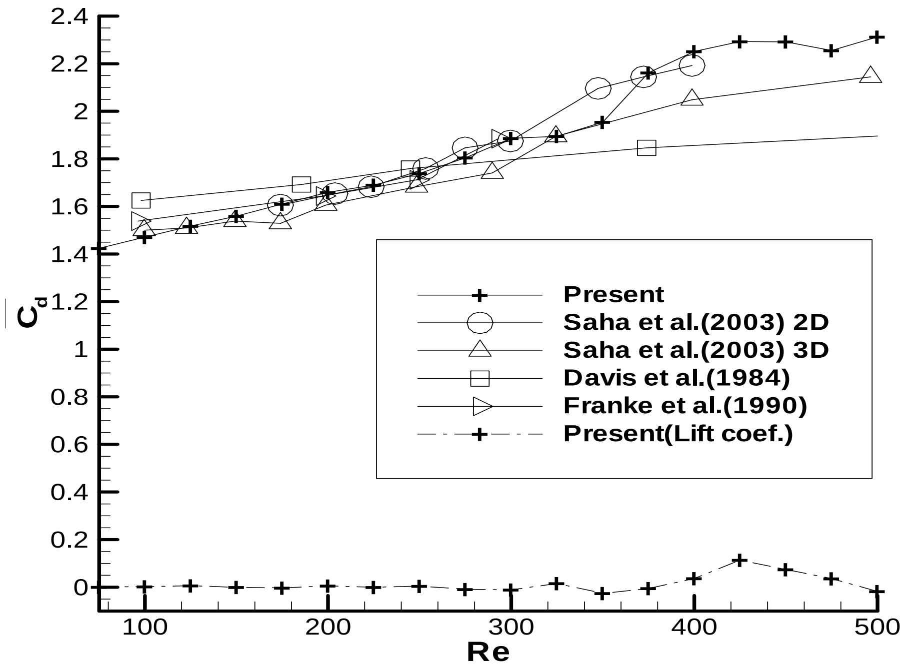

Figure 5-6. Variation of mean drag and lift coefficients with Reynolds number (Uniform free stream).

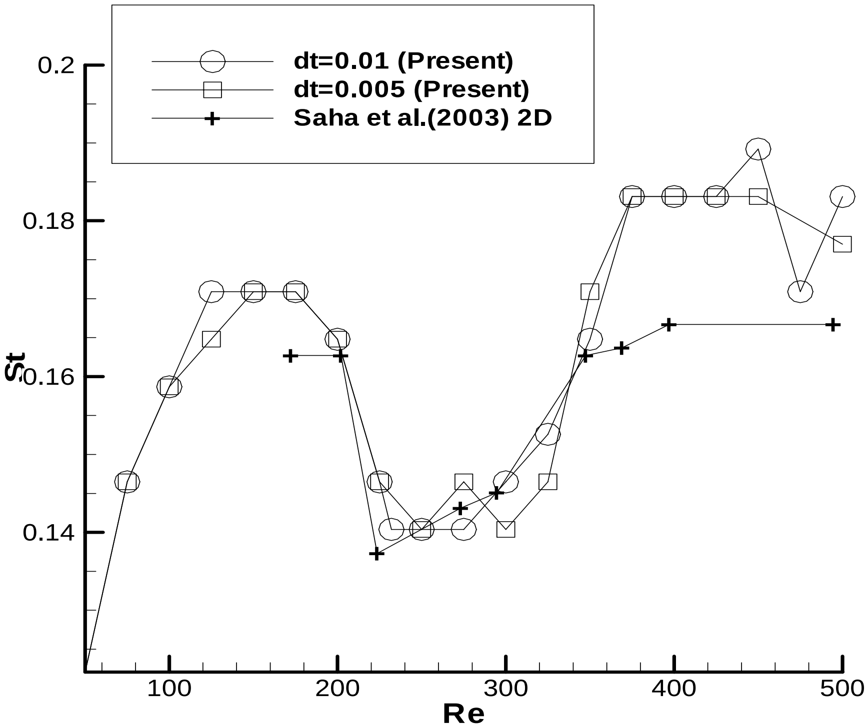

Figure 5-7. Variation of Strouhal number with Reynolds number (Uniform free stream cases of time step sizes 0.01 and 0.005).

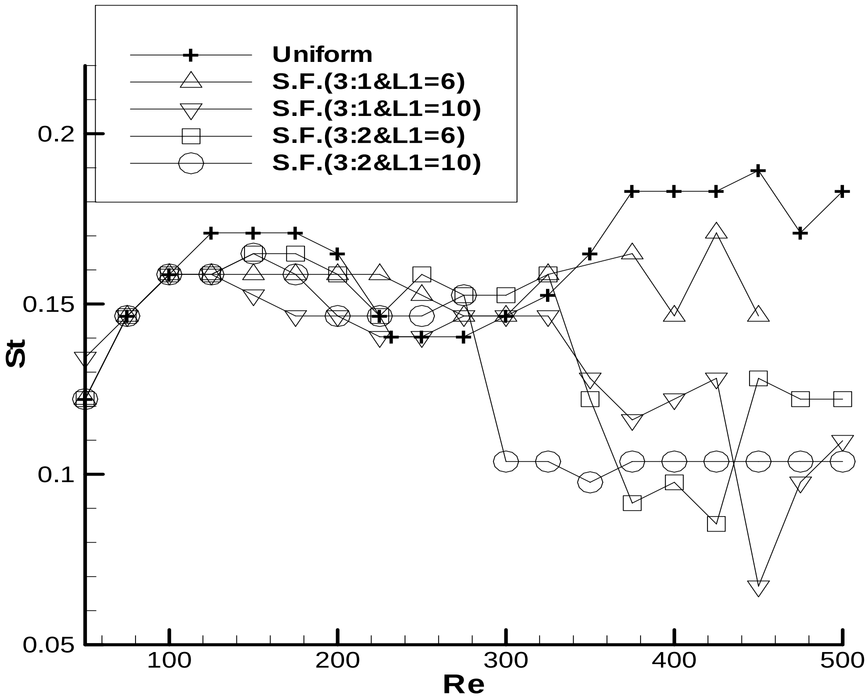

Figure 6-1. Variation of Strouhal number with Reynolds number (Uniform and shear free streams).

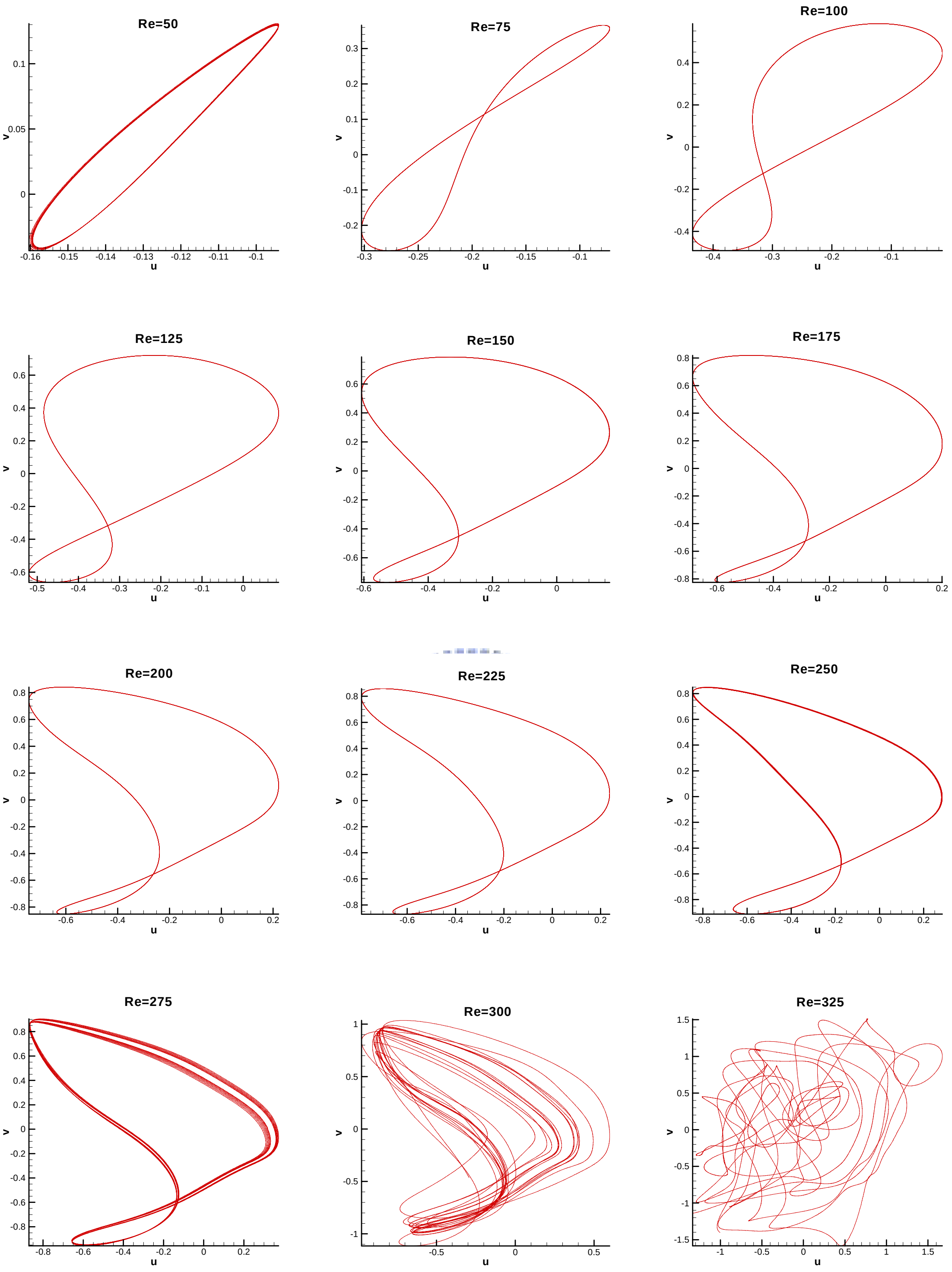

Figure 6-2. Variation of phase space of velocity components at (x=1.23, y=0) with Reynolds number (Velocity ratio 3:1 and L1=6). *Continue…*